Article

Discovery Medicine 2026; 38(206): 778–788
https://doi.org/10.24976/Discov.Med.202638206.64

SREBF2 Depletion From MDFI Enhancers Suppresses Keloid Fibroblast Hyperproliferation by Engaging a Molecular "Brake"

Chanli Wu[1], CHIEN-YOU Huang[1,*]

[1]Dermatology Department, Wu's Logic Aesthetics Clinic, 104 Taipei, Taiwan
*Correspondence: huangqianyou_HQY@163.com (CHIEN-YOU Huang)
Submitted: 3 November 2025 Revised: 30 January 2026 Accepted: 25 February 2026 Published: 20 March 2026

Background: Keloid disorder manifests as the hyperproliferation of fibroblasts and resultant excessive scar formation, and the upregulation of the MyoD family inhibitor (MDFI) has been identified in keloids. Bioinformatics predictions further suggested an enrichment of sterol regulatory element binding transcription factor 2 (SREBF2) at the MDFI enhancer site. This study aimed to elucidate the specific roles and the potential regulatory axis of SREBF2 and MDFI in the proliferation of keloid fibroblasts (KFs).

Methods: The location of MDFI enhancer was predicted through bioinformatics. Chromatin immunoprecipitation followed by polymerase chain reaction was subsequently performed to quantify the enrichment of histone H3 lysine 27 acetylation (H3K27Ac) and SREBF2 at the MDFI enhancer in KFs derived from keloid dermis or normal skin fibroblasts (NFs) collected from adjacent healthy skin tissues. Following transfection as appropriate, proliferation, migration and invasion of KFs were determined through Ki67 staining, wound healing assay and Transwell assay, respectively. Western blot or quantitative real-time reverse transcription PCR analyses were applied to test the expression levels of MDFI, SREBF2, or apoptosis-related proteins (BCL2 associated X (Bax), BCL2 apoptosis regulator (Bcl-2)).

Results: MDFI and SREBF2 expression levels were upregulated in keloid dermis ($p < 0.05$). SREBF2 was enriched in the enhancer region of MDFI, and its silencing suppressed MDFI expression in KFs ($p < 0.05$). MDFI overexpression promoted proliferation, migration and invasion, elevated Bcl-2 expression in KFs, but suppressed Bax expression, whereas MDFI silencing did conversely ($p < 0.05$). SREBF2 silencing repressed proliferation, migration and invasion, diminished Bcl-2 expression in KFs, but augmented Bax expression, which was counteracted by overexpressed MDFI ($p < 0.05$).

Conclusion: This study demonstrates that SREBF2 promotes KF proliferation, migration and invasion, and inhibits apoptosis by activating MDFI through binding to MDFI enhancer transcription. The identified SREBF2/MDFI axis presents a novel potential therapeutic target for mitigating keloid progression.

Keywords: sterol regulatory element binding transcription factor 2; MyoD family inhibitor; enhancer; fibroblast; keloid

Introduction

Keloids are a cutaneous fibroproliferative disorder, pathologically characterized by excessive proliferation of fibroblasts and massive deposition of extracellular matrix [1–4]. The causative factors of keloid include herpes zoster infection, burns, local trauma, and surgery. [5]. Clinically, the treatment of keloid is challenging due to its high recurrence, extracellular matrix formation and fibroblast hyperproliferation [6,7]. Hence, the research targeting these processes is of great significance to further elucidate the pathogenesis of keloid and benefit the clinical treatment of keloid.

In the past decade, the hyperproliferation of keloid fibroblasts (KFs) has garnered much attention due to its irreplaceable role in the progression of keloid [8,9]. The fibroblast hyperproliferation has been considered as one of the main pathophysiologies in keloids [10,11], but its precise underlying mechanisms in keloids still remain unexplored. Therefore, this study probed into the potential key genes involved in the regulation of KF hyperproliferation. As a transcription factor, MyoD family inhibitor (MDFI) primarily mediates the activity of myogenic family proteins [12]. Also, MDFI plays an essential role in several diseases, and acts as a potential biomarker in various cancers, including lung adenocarcinoma [13] and colorectal cancer [14]. MDFI (I-mfa) has been shown to promote the fibronectin production stimulated by TGF-β1 in human mesangial cells (MCs), potentially at the transcriptional level [15]. Accumulating evidence has revealed that fibronectin is involved in the progression of keloid, underscoring it as a promising target for the therapeutic strategy development [16]. Besides, MDFI has been proven to be expressed in both cultured cells and keloid tissues, suggesting its possible in-

volvement in the pathology of primary keloid [6]. Hence, we selected MDFI as the candidate gene to further investigate its association with KF hyperproliferation.

Furthermore, given MDFI's role as a transcriptional modulator, we focused on transcriptional enhancers. As previously described, enhancers are DNA sequences, typically 200–1500 base pairs in length, that regulate gene expression. They contain sequence-specific binding sites for transcription factors, which recognize and bind to these sequences, thereby initiating the transcription of target genes. To identify potential regulators of MDFI, the location of its enhancer was predicted using the SEdb database. Remarkably, we found the transcription factor, sterol regulatory element binding transcription factor 2 (SREBF2), as enriched within the region of MDFI enhancer. SREBF2 is well-known for its role in lipid and cholesterol homeostasis, and is related to hepatic steatosis and hypercholesterolemia [17]. Moreover, SREBF2 suppression can inhibit the skin inflammation in psoriasis [18]. Given the shared features of dysregulated cell proliferation and inflammation in psoriasis and keloid, we hypothesized that SREBF2 might also contribute to keloid formation and sought to investigate its underlying mechanism and potential regulation of MDFI.

Collectively, the major aim of the present study is to explore the involvement of MDFI in the proliferation of KFs. Additionally, based on the bioinformatic predictions and the aforementioned hypothesis, we explored whether the enrichment of SREBF2 on MDFI enhancers is implicated in regulating the proliferation of KFs.

Methods

Ethics Statement

Keloid and adjacent normal skin tissue samples were available from 44 patients who underwent keloid resection surgery in Wu's Logic Aesthetics Clinic. Patient recruitment and sample collection were performed at Wu's Logic Aesthetics Clinic between January 2024 and December 2024. This study was conducted in accordance with the principles outlined in the Declaration of Helsinki. All patients have signed informed consent before the surgery. The study protocol has been reviewed and approved by the Ethics Committee of Wu's Logic Aesthetics Clinic ((Research) 2025- Ethics Approval -123).

Inclusion and Exclusion Criteria

The inclusion criteria were as follows: (1) patients $\geq$18 years old; (2) clinically diagnosed with keloids requiring surgical resection; and (3) willingness to provide written informed consent for the use of their tissue samples for research.

The exclusion criteria were as follows: (1) a history of radiotherapy at the keloid site; (2) administration with intralesional corticosteroid or other anti-keloid therapy within 3 months prior to surgery; (3) presence of active skin infections or systemic inflammatory diseases; (4) pregnant or lactating women; and (5) a known history of coagulation disorders or immunodeficiency.

Isolation and Culture of KFs and Normal Skin Fibroblasts (NFs)

In this study, KFs and NFs were isolated from the keloid dermis and adjacent normal skin tissues from 30 patients [19]. More specifically, the obtained specimens were cut into pieces (2–3 cm) and washed with ice-cold phosphate-buffered saline (PBS, abs962, Absin, Shanghai, China). Subsequently, Dispase II (D6430, Solarbio, Beijing, China) was dissolved in HEPES buffer saline (H1070, Solarbio, China) and diluted in Dulbecco's modified Eagle's medium (DMEM, 11966-025, Thermo Fisher Scientific, Waltham, MA, USA) to a final concentration of 3 mg/mL. Then, the tissue samples were incubated with 3 mg/mL Dispase II in DMEM for 1 h at 37 °C under 5% CO_2. Next, collagenase I (C8140, Solarbio, China) was dissolved in TESCA buffer (G0150, Solarbio, China) and diluted in DMEM to a final concentration of 1 mg/mL. After discarding the epidermis, the dermis was minced and digested with 1 mg/mL collagenase I in DMEM for 2.5 h at 37 °C. The resulting cell suspension was filtered through a 70-µm cell strainer and centrifuged. Following the removal of supernatant, the cells were cultured in DMEM supplemented with 10% fetal bovine serum (FBS, S9030, Solarbio, China) and 1% penicillin-streptomycin (60162ES76, Yeason, Shanghai, China) at 37 °C in a humidified atmosphere containing 5% CO_2. All cells were tested negative for mycoplasma. The identity of primary KFs and NFs was confirmed based on their characteristic morphology under a microscope and by immunofluorescence staining for fibroblast-specific markers-Vimentin. Based on the specific epigenetic activation identified in KFs, all subsequent functional experiments were performed using these KF cells.

Immunofluorescence Staining

Briefly, NFs and KFs cells grown on glass coverslips were fixed with 4% paraformaldehyde for 15 minutes at room temperature, followed by permeabilization with 0.1% Triton X-100 for 10 minutes. After blocking with 5% bovine serum albumin (BSA) for 1 hour, the cells were incubated overnight at 4 °C with a primary antibody against Vimentin (2 µg/mL, ab92547, Abcam, UK). Subsequently, cells were incubated with an appropriate fluorophore-conjugated secondary antibody against Rabbit IgG (1:1000, ab99697, Abcam, UK) for 1 hour at room temperature in the dark. Cell nuclei were counterstained with 4′,6-diamidino-2-phenylindole (DAPI) (abs47047616, Absin, China). Finally, the coverslips were mounted onto glass slides, and images were captured using a fluorescence microscope (Olympus, Tokyo, Japan).

Cell Transfection

The small interfering RNA targeting MDFI (siMDFI, forward, 5′-AUUUUUCUGUCCUCUAAGCCU-3′; reverse, 5′-GCUUAGAGGACAGAAAAAUGU-3′), SREBF2 (siSREBF2, forward, 5′-UCAUUACCGUCUGUUGUUGCA-3′; reverse, 5′-CAACAACAGACGGUAAUGAUC-3′) and their negative control (siNC, forward, 5′-UUCUCCGAACGUGUCACGU-3′; reverse, 5′-ACGUGACACGUUCGGAGAA-3′) were constructed using GenePharma (Shanghai, China). Meanwhile, the sequence of MDFI was amplified and ligated onto pcDNA3.1 vectors (VT1001, YouBio, Changsha, China) for the corresponding overexpression plasmids, while its NC (5′-CTAGAGAACCCACTGCTTAC-3′) was also obtained. The coding sequence (CDS) region of MDFI was provided in the supplementary materials. Then, the lipofectamine™ 3000 transfection reagent (L3000015, Thermo Fisher Scientific, USA) was used for corresponding transfection after the cell confluence reached 90% in a 96-well plate. In detail, the Lipofectamine™ 3000 reagent, siRNA, and overexpression plasmids were diluted in the Opti-MEM™ medium (31985062, Thermo Fisher Scientific, USA). After that, plasmids were mixed with P3000 reagent, and siRNA/plasmids were added into the tubes and incubated with diluted lipofectamine™ 3000 transfection reagent for 10 min at room temperature. Finally, gene-lipid complexes were added to each well and incubated for another 48 h at 37 °C.

Bioinformatics

SEdb 2.0 (http://www.licpathway.net/sedb/) was employed to predict the location of MDFI enhancer and its binding relation with transcription factors.

Chromatin Immunoprecipitation-qPCR (ChIP-qPCR) Analysis

In brief, KFs and NFs were firstly cross-linked using 1% formaldehyde (F8775, Sigma-Aldrich, Darmstadt, Germany) for 10 min at room temperature, lysed with lysis buffer (#9803, Cell Signaling Technology, Danvers, MA, USA), and centrifuged at 2500 ×g for 10 min. Afterwards, the resulting supernatant was harvested and incubated with the antibodies against either control IgG (26156, Thermo Fisher Scientific, USA), or SREBF2 (1:200, #25940, Cell Signaling Technology, Danvers, MA, USA)/histone H3 lysine 27 acetylation (H3K27Ac, 1:100, ab4729, Abcam, UK) at 4 °C overnight. Then, the protein agarose was employed to precipitate the compound of endogenous DNA-protein, which was de-crosslinked at 65 °C overnight. Finally, the DNA fragments were extracted, purified, and recycled with phenol/chloroform (AK169, MREDA, Beijing, China), and the enrichment of SREBF2/H3K27Ac was evaluated via quantitative real-time reverse transcription PCR (qRT-PCR) [20].

The PCR sequences used in this part were shown as follows: MDFI (5000 bp upstream): forward, 5′-GCATCCCCGAAATCTTGCAC-3′; reverse, 5′-ATTCCAAGTCGCCTGCTTGA-3′. MDFI (5000 bp downstream): forward, 5′-CAAGTAGCTGAACCAGGGGG-3′; reverse, 5′-CAGCAGTTGGCCTGAAAACC-3′. MDFI (enhancer): forward, 5′-AAGGTAAGCACCCATCCCATC-3′; reverse, 5′-GTGTTGTAGGCACATCGGCT-3′.

Dual-Luciferase Reporter Assay

After KF cells were cultured in 96-well plates for 24 h, the MDFI-Wide-type (WT, 5′-AAAACGTGAC-3′) or MDFI-mutant (MUT, 5′-AAAAATTGAC-3′) luciferase vector sequence was amplified and inserted into pGL3 vector (E1751, Promega, USA). These constructs were then co-transfected with either siSREBF2 or a negative control siRNA (siNC) into the cells using Lipofectamine 3000 reagent. Finally, the luciferase activity of the cells was detected on the Luc-Screen™ Extended-Glow Luciferase Reporter Gene Assay System (T1033, Thermo Fisher, USA), and data were analysed on a chemiluminescence analyser (1410130, Thermo Fisher, USA).

qRT-PCR

Total RNA from keloid dermis, adjacent normal skin tissues, and KFs/NFs was extracted with RNeasy mini kit (74104, Qiagen, Hilden, Germany). Later, PrimeScript™ RT reagent kit (RR037A, TaKaRa, Beijing, China) was employed to synthesize total RNA into complementary DNA (cDNA), after which qRT-PCR was performed on an ABI 7500 System (ABI 7500, Thermo Fisher Scientific, USA) using 2× SYBR Green qPCR Master Mix (B21203, Bimake, Houston, TX, USA) at the indicated conditions: 40 cycles at 95 °C for 15 s, 55 °C for 30 s and 72 °C for 30 s. The $2^{-\Delta\Delta Ct}$ method [21] was used to calculate the expression levels of corresponding genes.

The PCR sequences were as follows: SREBF2: forward, 5′-CAGCAGGTGCAGACAGTACA-3′; reverse, 5′-TCTGGATAGGGGTGGTGAGG-3′. MDFI: forward, 5′-TTGCAGAGTTTGGACAGGCA-3′; reverse, 5′-CCCAGGAAGGAGGGATAGGG-3′. Glyceraldehyde-3-phosphate dehydrogenase (GAPDH) (internal loading control): forward, 5′-TCAGCCGCATCTTCTTTTGC-3′; reverse, 5′-ATGGTGTCTGAGCGATGTGG-3′.

Ki67 Staining

Briefly, KFs were fixed in 4% paraformaldehyde (P1110, Solarbio, China) at room temperature for 20 min, and permeabilized with 0.1% Triton X-100 (X100, Sigma-Aldrich, Germany) in PBS for 5 min. Afterwards, the cells were blocked with serum for 20 min and incubated with primary antibody, Alexa Fluor 594-conjugated Ki-67 (#33908, Cell Signaling Technology, USA) overnight at 4 °C. DAPI solution (abs47047616, Absin, China) was used

to achieve nuclear staining for 5 min in the dark. Subsequently, Ki67-positive cells were tested through a BX63 fluorescence microscope (Olympus, Tokyo, Japan) at ×200 magnification. Ki67 proliferation rate (%) = (Number of Ki67–positive cells / Number of total cells) × 100.

Wound Healing Assay

KFs were seeded in the 6-well plates at the density of 1 × 10^5 cells/well. Then, an artificial wound was created on the monolayers once cells became fully confluent. Following 24-h incubation in the culture media without serum, the debris of these cells was removed by cotton swabs, and the cells were observed under a DP27 inverted optical microscope (Olympus, Japan) at ×100 magnification. Relative migration rate (%) = (Wound closure of treatment group) / (Wound closure of control group) × 100.

Transwell Assay

A Transwell chamber (8.0-µm pore size, CLS3464, Corning Life Sciences, Corning, NY, USA) was used to conduct the invasion assay as needed. In detail, 60 µL Matrigel (356234, Solarbio, China) was pre-coated on the upper chamber while KFs (1 × 10^5) were resuspended in the DMEM without serum on the upper chamber. Thereafter, DMEM (500 µL) with 10% FBS was added into the lower chamber. Following 24-h incubation, the Matrigel and the cells on the upper chamber were removed by cotton swabs. Cells in the lower chambers were fixed with 4% paraformaldehyde for 10 min at room temperature, and stained with crystal violet (abs817172, Absin, China) for 30 min. After the PBS washing, the invasive cells were observed under the microscope at ×250 magnification. Relative invasion rate (%) = (Number of invaded cells in treatment group) / (Number of invaded cells in control group) × 100.

Western Blotting

The total protein was isolated from KFs through RIPA Lysis Buffer (E-BC-R327, Elabscience, Wuhan, China), followed by concentration measurement using the BCA protein quantification kit (P0012S, Beyotime, Shanghai, China). Later, the protein samples were electrophorized in 12% sodium dodecyl sulfate polyacrylamide gel electrophoresis (SDS-PAGE) gels (P0672, Beyotime, China), and transferred onto polyvinylidene fluoride (PVDF) membranes (88585, Thermo Fisher Scientific, USA). The membranes were then blocked with 5% non-fat skim milk (D8340, Solarbio, China), pre-diluted in Tris Buffered Saline with Tween-20 (T1085, Solarbio, China) for 2 h at room temperature, incubated with primary antibodies, BCL2 associated X (Bax) (1:1000, ab32503, 21 kDa, Abcam, UK), BCL2 apoptosis regulator (Bcl-2) (1:1000, ab32124, 26 kDa, Abcam, UK), and GAPDH (1:1000, ab8245, 37 kDa, Abcam, UK), at 4 °C overnight, and further cultured with horseradish peroxidase (HRP) labeled secondary antibodies against Mouse IgG (1:2000, ab6728, Abcam, UK) and Rabbit IgG (1:1000, ab99697, Abcam, UK) for 1 h at room temperature.

Finally, the band signals were analyzed with ECL reagent kits (FP300, ABP Biosciences, Rockville, MD, USA) on Tanon 5200 imaging system (Shanghai, China), followed by quantitative analysis using ImageJ 5.0 (Bio-Rad, Hercules, CA, USA), and normalization to GAPDH (loading control). Data are expressed as fold change relative to the control group.

Flow Cytometry

Apoptosis was evaluated using the Annexin V-FITC Cell Apoptosis Kit (640914, BioLegend, USA). 24 h after treatment, cells were detached using Trypsin-EDTA (C0201, Beyotime, China) and neutralized with complete medium. Following centrifugation, the collected cells were washed with PBS, and the pellet was resuspended in 195 µL 1X binding buffer. Cells were incubated with 5 µL Annexin V-FITC and 10 µL propidium iodide (PI) (15 min, room temperature, darkness), and reacted with 400 µL of 1× binding buffer. With NovoCyte Penteon flow cytometer (Agilent, USA), the levels of FITC and PI fluorescence were detected, and early apoptotic cells (Annexin V-positive and PI-negative) and late apoptotic cells (positive for both markers) were identified.

Statistical Analyses

All data were expressed as mean ± standard deviation (SD) and analyzed in GraphPad Prism 8 (GraphPad, Inc., La Jolla, CA, USA). Data between two groups and among multiple groups were compared with the independent samples *t*-test or one-way analysis of variance, followed by Tukey's post hoc test. The statistical significance was defined when the *p*-value was below the threshold of 0.05.

Results

MDFI and SREBF2 Expression Levels were Upregulated in Keloid Dermis

Firstly, given the possible roles of MDFI and SREBF2 in keloid, their expression levels in keloid dermis or adjacent normal skin tissues were evaluated using qRT-PCR. As shown in Fig. 1A,B, MDFI and SREBF2 expression levels in keloid dermis were higher than those in the adjacent normal skin tissues ($p < 0.05$).

SREBF2 was Enriched in Region of the Enhancer MDFI and siSREBF2 Downregulated MDFI Expression in KFs

The binding diagram of transcription factors and enhancer of MDFI was shown based on SEdb 2.0 database (Fig. 1C), predicting that SREBF2 was enriched in the region of MDFI enhancer. Under inverted microscopy, NFs and KFs presented distinct structures: NFs exhibited

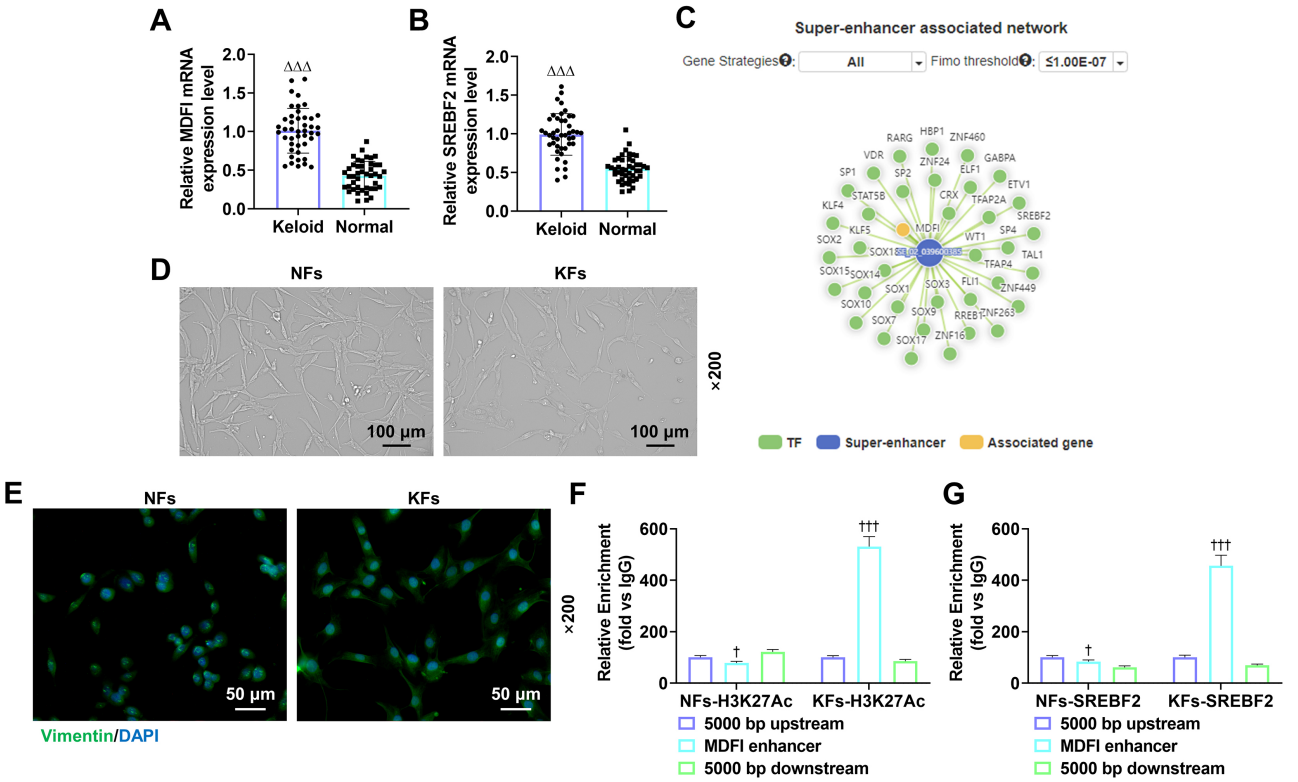

Fig. 1. MDFI and SREBF2 expression levels in keloid dermis, and enrichment of SREBF2 on MDFI enhancer in NFs/KFs. (A,B) The expression levels of MDFI and SREBF2 in keloid dermis or adjacent normal skin tissues were evaluated using qRT-PCR. GAPDH was used as a loading control. (C) The binding diagram of transcription factors and the enhancer of MDFI was shown based on SEdb 2.0 database. (D) Morphological observation of normal skin fibroblasts (NFs) and keloid fibroblasts (KFs) under a microscope (×200 magnification, scale bar: 100 μm). (E) Identification of NFs and KFs by immunofluorescence staining for Vimentin (×200 magnification, scale bar: 50 μm). (F,G) ChIP-qPCR was used to measure the enrichment of H3K27Ac/SREBF2 on 5000 bp upstream/downstream region of the enhancer MDFI or the MDFI enhancer in NFs/KFs. $^{\Delta\Delta\Delta}p < 0.001$ vs. Normal; $^{\dagger}p < 0.05$, $^{\dagger\dagger\dagger}p < 0.001$ vs. 5000 bp upstream. Abbreviation: MDFI, MyoD family inhibitor; SREBF2, sterol regulatory element binding transcription factor 2; NFs, normal skin fibroblasts; KFs, keloid fibroblasts; qRT-PCR, quantitative real-time reverse transcription polymerase chain reaction; GAPDH, glyceraldehyde-3-phosphate dehydrogenase; ChIP-qPCR, Chromatin immunoprecipitation-qPCR; H3K27Ac, histone H3 lysine 27 acetylation.

a braided vortex pattern with orderly arrangement, while KFs displayed spindle-shaped radial organization (Fig. 1D). Immunofluorescence staining further confirmed the fibroblastic identity of both cell types, as they exhibited strong positivity for Vimentin. Additionally, both cell types exhibited typical elongated fusiform morphology and demonstrated active proliferation (Fig. 1E). It has been acknowledged that H3K27ac serves as a marker for the enhancers [22]. Herein, the results of ChIP-qPCR suggested that, in NFs, the enrichment of H3K27Ac/SREBF2 at the MDFI enhancer was significantly lower than that at the 5000 bp upstream region of the MDFI enhancer (Fig. 1F,G, $p < 0.05$). In contrast, in KFs, the enrichment of H3K27Ac/SREBF2 on the MDFI enhancer was significantly higher than that at the corresponding 5000 bp upstream region (Fig. 1F,G, $p < 0.05$). These findings confirmed that theMDFI enhancer was activated in KFs and was associated with SREBF2 enrichment. Then, siMDFI, overexpression plasmid of MDFI, or siSREBF2 was transfected into KFs. Transfection efficiency was confirmed by the decreased/increased MDFI expression (Fig. 2A, $p < 0.05$) and reduced SREBF2 expression in the cells (Fig. 2B, $p < 0.05$). Additionally, as shown in Fig. 2B, siSREBF2 treatment led to the down-regulation of MDFI expression in KFs ($p < 0.05$). The subsequent results of ChIP-qPCR revealed that siSREBF2 reduced SREBF2 enrichment at both the MDFI enhancer and its 5000 bp upstream/downstream regions (Fig. 2C, $p < 0.05$). Also, the relative luciferase activity was reduced in KFs co-transfected with the MDFI-WT reporter and siSREBF2 (Fig. 2D, $p < 0.05$).

MDFI Promoted Proliferation, Migration and Invasion, while Suppressing Apoptosis of KFs

Meanwhile, we investigated the roles of MDFI in proliferation of KFs. In accordance with the results of Ki67 staining, overexpressed MDFI increased the number

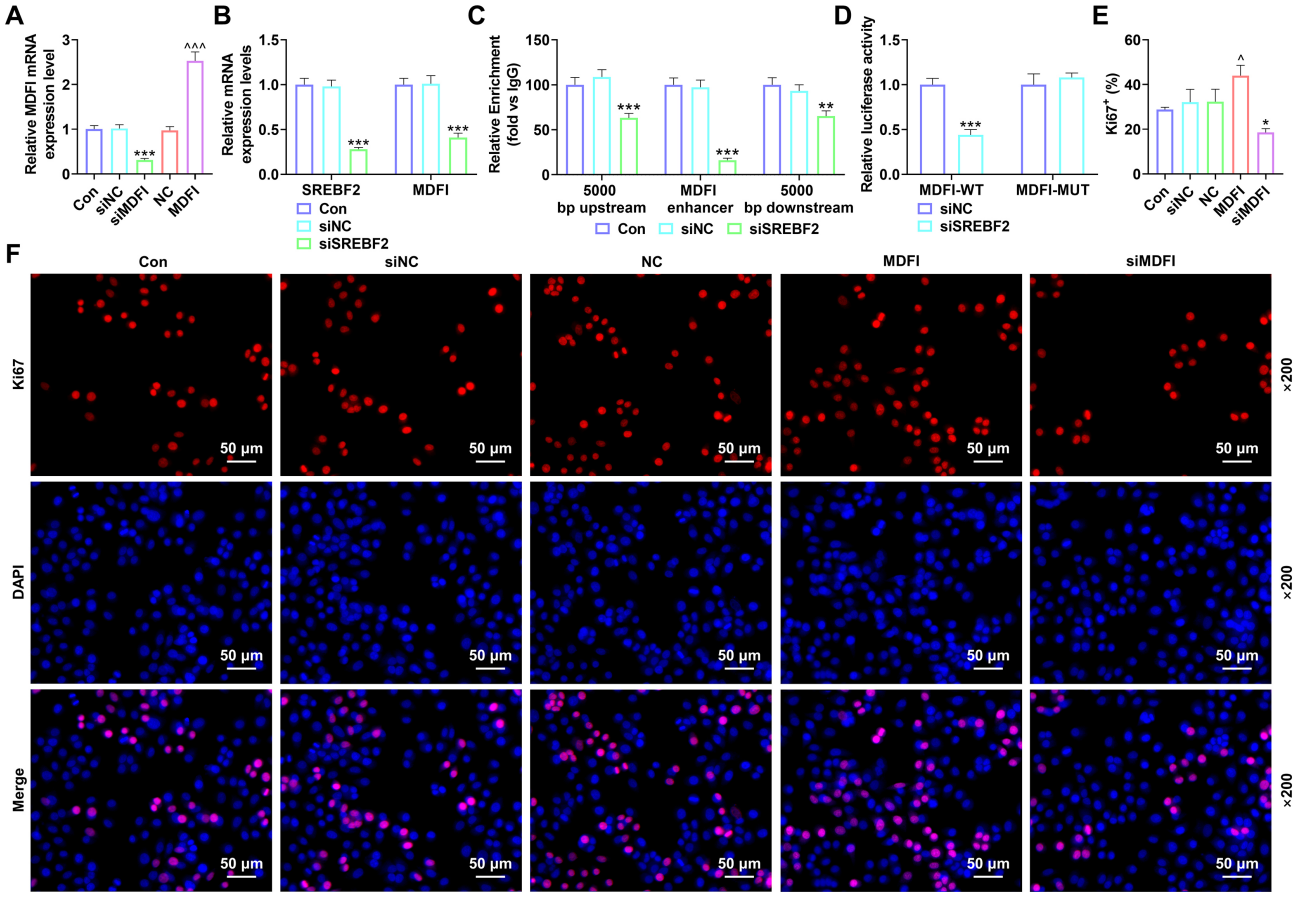

Fig. 2. Effects of siMDFI/overexpressed MDFI on enrichment of SREBF2 in the region of the MDFI enhancer and proliferation of KFs. (A,B) After siMDFI, siSREBF2, or overexpression plasmid of MDFI was transfected into KFs, MDFI/SREBF2 expression was evaluated in the cells by qRT-PCR. GAPDH was used as a loading control. (C) Following the transfection of siSREBF2 in KFs, ChIP-qPCR was employed to measure SREBF2 enrichment at both the MDFI enhancer and its 5000 bp upstream/downstream region. (D) Dual-luciferase reporter assay was used to validate the binding of SREBF2 to the MDFI enhancer. (E,F) After the transfection of siMDFI and overexpression plasmid of MDFI in KFs, Ki67 staining was used to evaluate the proliferation of KFs (scale: 50 μm; magnification: ×200). $^{*}p < 0.05$, $^{**}p < 0.01$, $^{***}p < 0.001$ vs. siNC. $^{\wedge}p < 0.05$, $^{\wedge\wedge\wedge}p < 0.001$ vs. NC. Abbreviation: Con, control (untreated cells); siMDFI, small interfering RNA targeting MDFI; siSREBF2, small interfering RNA targeting SREBF2; siNC, small interfering RNA negative control; NC, negative control.

of Ki67-positive cells (Fig. 2E,F, $p < 0.05$), whereas the siMDFI exerted an opposite effect (Fig. 2E,F, $p < 0.05$), implying that MDFI boosted the proliferation of KFs. Besides, the results of wound healing assay (Fig. 3A,C) and Transwell assay (Fig. 3B,D) demonstrated that overexpressed MDFI elevated the migration/invasion rate in KFs ($p < 0.05$), but siMDFI resulted in opposite trends ($p < 0.05$). In light of previous research, the Bcl-2 protein family plays a central role in the process of apoptosis, comprising pro-apoptotic proteins (such as Bax) and anti-apoptotic proteins (such as Bcl-2) [23]. According to the data of Western blotting (Fig. 3E–G), overexpressed MDFI downregulated Bax and upregulated Bcl-2 in KFs ($p < 0.05$), whilst siMDFI generated opposite effects on Bcl-2 and Bax expression levels ($p < 0.05$). Flow cytometry outcomes showed that MDFI overexpression reduced, while MDFI silencing increased apoptosis rate (Fig. 3H,I, $p < 0.05$). Accordingly, we inferred that MDFI inhibited the apoptosis of KFs.

SiSREBF2 Decreased Proliferation, Migration and Invasion, and Increased Apoptosis in KFs, which were all Counteracted by Overexpressed MDFI

Moreover, the subsequent results of Ki67 staining (Fig. 4A,B), wound healing assay (Fig. 4C,D) and Transwell assay (Fig. 5A,B) suggested that siSREBF2 decreased the number of Ki67-positive cells, migration rate, and invasion rate in KFs ($p < 0.05$). Importantly, the expression levels of these aforementioned factors were increased in KFs following transfection with the MDFI overexpression plasmid (Fig. 4, Fig. 5A,B, $p < 0.05$). Regarding apoptosis, siSREBF2 significantly elevated Bax expression and reduced Bcl-2 expression in KFs (Fig. 5C–E, $p < 0.05$), which was

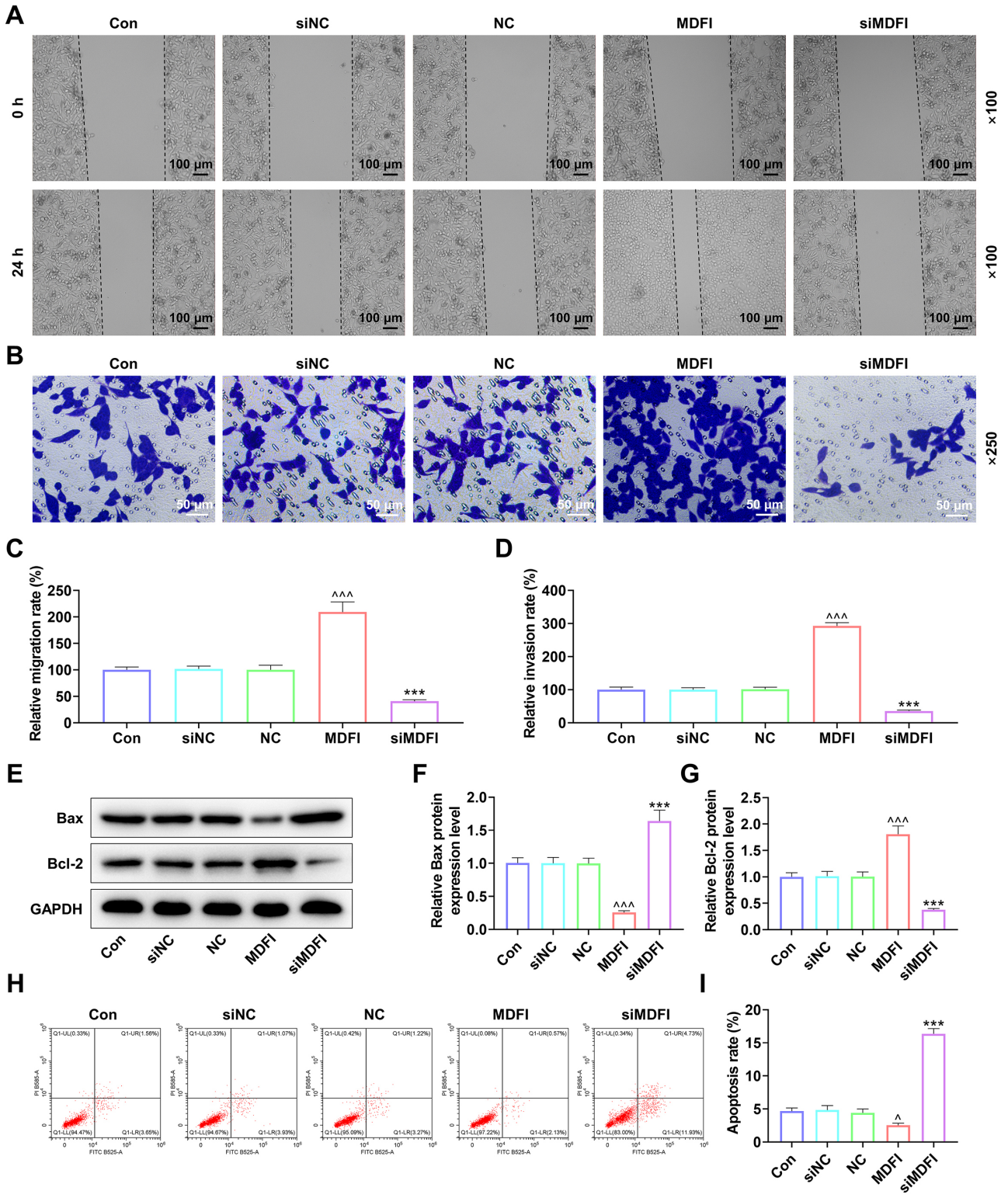

Fig. 3. Effects of siMDFI/overexpressed MDFI on migration, invasion, and apoptosis in KFs. (A–D) After the transfection of siMDFI and overexpression plasmid of MDFI in KFs, (A,C) migration of the cells was tested via the wound healing assay (scale: 100 μm; magnification: ×100), and (B,D) invasion of the cells was tested via Transwell assay (scale: 50 μm; magnification: ×250). (E–G) After transfection, Bcl-2 and Bax expression levels in KFs were assessed via Western blotting. GAPDH was used as a loading control. (H,I) The apoptosis of KF cells was detected using flow cytometry. $^{***}p < 0.001$ vs. siNC. $^{\wedge}p < 0.05$, $^{\wedge\wedge\wedge}p < 0.001$ vs. NC. Abbreviation: Bcl-2, BCL2 apoptosis regulator; Bax, BCL2 associated X.

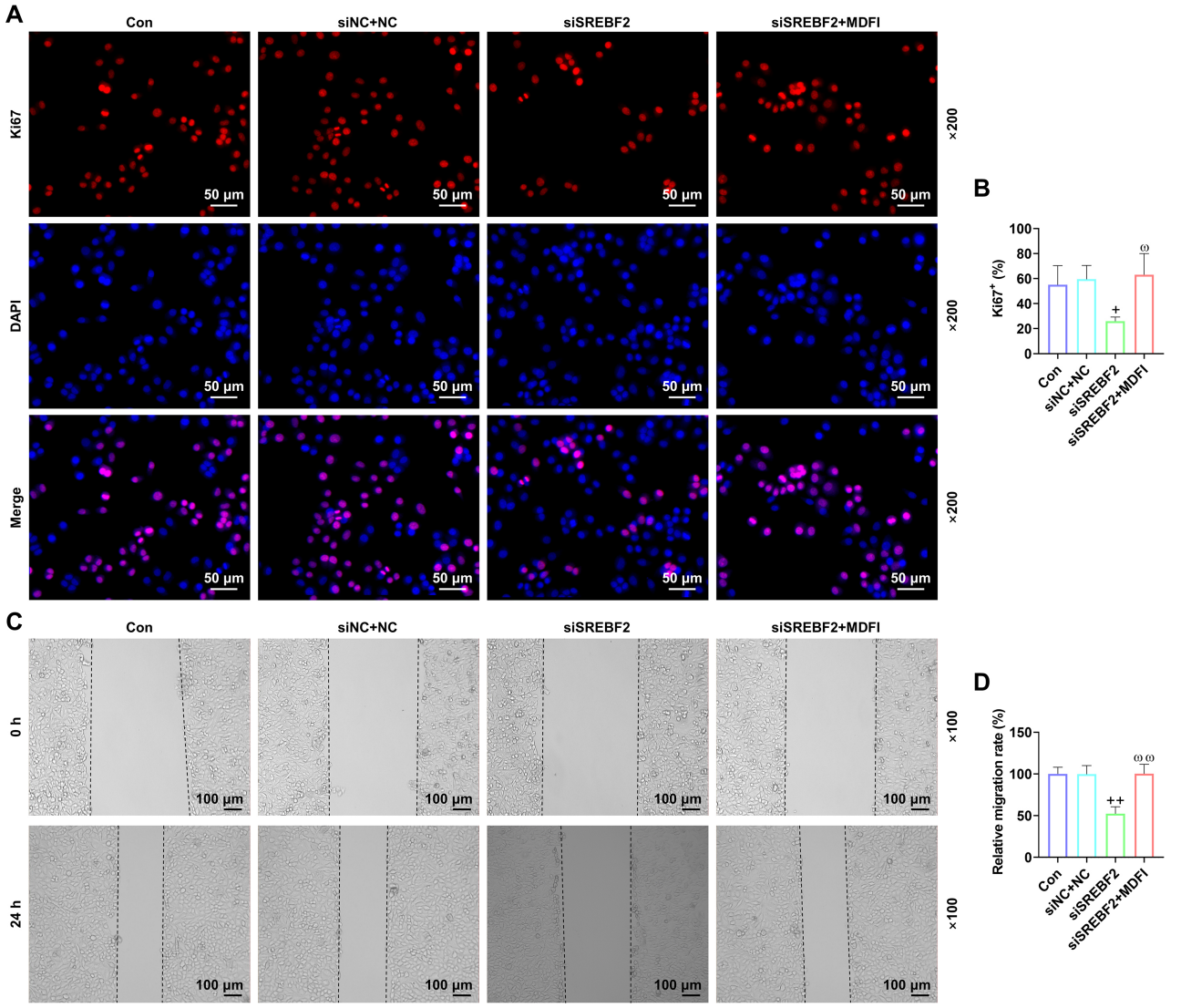

Fig. 4. Effects of siSREBF2/overexpressed MDFI on proliferation and migration in KFs. (A,B) After the transfection of siSREBF2/overexpression plasmid of MDFI in KFs, Ki67 staining was used to measure the proliferation of the cells (scale: 50 μm; magnification: ×200). (C,D) After transfection, wound healing assay was applied to determine the migration of KFs (scale: 100 μm; magnification: ×100). $^{+}p < 0.05$, $^{++}p < 0.01$ vs. siNC+NC. $^{\omega}p < 0.05$, $^{\omega\omega}p < 0.01$ vs. siSREBF2.

offset by transfection with the MDFI overexpression plasmid ($p < 0.05$). Flow cytometry results showed that siSREBF2 promoted apoptosis, while MDFI overexpression reversed the effects of siSREBF2 (Fig. 5F,G, $p < 0.05$).

Discussion

Keloids are characterized by a high recurrence rate, impose a substantial burden on human health, and seriously affect the quality of life of patients. In the present study, we identified MDFI as a potential candidate regulator of KF proliferation. Previous research has revealed that MDFI is upregulated in the keloid lesions, and MDFI-positive cells are present in keloid-associated lymphoid tissues, suggesting its involvement in the pathogenesis of keloid [6]. Consistent with this previous finding, we also confirmed that MDFI expression is upregulated in keloid dermis.

Reportedly, increased proliferation of fibroblasts is a well-established hallmark of keloid progression [24–26], accompanied by decreased apoptosis, leading to fibroblast invasion into adjacent normal skin tissues [27,28]. These observations suggest that the corresponding genes regulating fibroblast proliferation and may serve as potential therapeutic targets. Currently, MDFI has been proven to participate in various diseases, including lung adenocarcinoma [13] and gastric cancer [29], and its role as a tumor modulator in cancers has also been verified [30]. MDFI plays an active role in the differentiation of C2C12 cells [12], and its deficiency can inhibit the proliferation of gastric cancer cells [31]. More importantly, growing evidence indi-

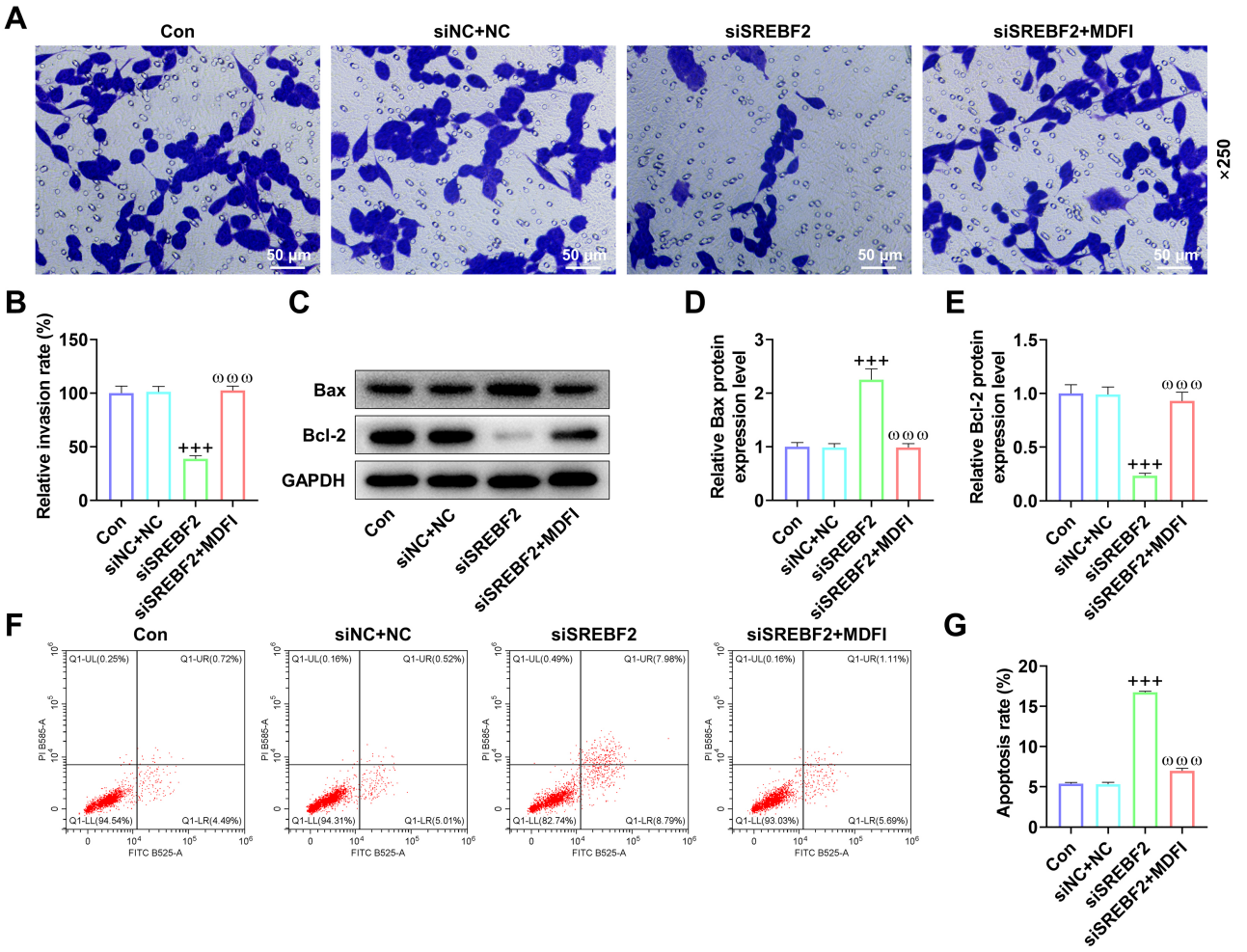

Fig. 5. Effects of siSREBF2/overexpressed MDFI on invasion and apoptosis in KFs. (A,B) After the transfection of siSREBF2/overexpression plasmid of MDFI in KFs, invasion of the cells was measured via Transwell assay (scale: 50 μm; magnification: ×250). (C–E) After transfection, Bcl-2 and Bax expression levels in KFs were determined via Western blotting. GAPDH was used as a loading control. (F,G) The apoptosis of KF cells was detected using flow cytometry. $^{+++}p < 0.001$ vs. siNC+NC. $^{\omega\omega\omega}p < 0.001$ vs. siSREBF2.

cates that the MDFI-positive cells show fibroblastic features and are localized in keloid-associated lymphoid tissues [6]. Thus, we investigated whether MDFI was involved in the regulation of fibroblast proliferation in keloid. Following the transfection with an MDFI overexpression plasmid or siMDFI, we observed that MDFI promoted the proliferation of KFs cells, concomitant with the enhanced migratory and invasive capacities. Moreover, apoptosis is an integral part of various cellular metabolic processes in mammals, which is implicated in normal cell renewal, development and functional maintenance of the immune system, embryonic development and cell death induced by external factors [32]. Bcl-2 protein family is instrumental in the process of apoptosis, which consists of pro-apoptotic proteins (e.g., Bax) and anti-apoptotic proteins (e.g., Bcl-2) [23]. Based on the expression profiles of Bcl-2 and Bax in KFs, we further proved that MDFI suppressed apoptosis of KFs. Collectively, these results establish MDFI as a promoter of KF proliferation and a key regulator contributing to the hyperproliferation that drives keloid progression.

SREBF2 is a well-established critical regulator of lipid metabolism, primarily controlling cholesterol homeostasis and contributing to fatty acid synthesis [17]. However, its role in keloid pathogenesis, particularly in fibroblast proliferation, remains largely unexplored. Herein, we found that SREBF2 is upregulated in keloid tissues and enriched at the MDFI enhancer in KFs, suggesting a non-canonical function beyond lipid metabolism. Moreover, with overexpressed MDFI and siSREBF2, we indicated that siSREBF2 suppresses KF proliferation, along with reduced SREBF2 enrichment on the MDFI enhancer and downregulated MDFI in KFs. Based on these findings, it can be inferred that reduced enrichment of SREBF2 at the MDFI enhancer negatively regulates KF proliferation. Ad-

ditionally, overexpressed MDFI counteracts the role of siSREBF2 in KFs, signifying that SREBF2 enrichment inhibition on MDFI enhancer dampens the hyperproliferation of KFs. This SREBF2-MDFI regulatory axis represents a novel pathway contributing to keloid pathogenesis. While SREBF2 is classically activated by sterol depletion, its specific recruitment to the MDFI enhancer in KFs may involve cell-type-specific co-factors or chromatin states, potentially linking local metabolic changes to fibroproliferative responses. However, this study has not yet clarified the upstream mechanism by which SREBF2 is specifically recruited to the MDFI enhancer. This process may rely on its classic activating partner SCAP and cholesterol signaling, but it may also involve synergistic effects with other transcription factors in KFs. Analyzing this precise recruitment mechanism will be the central focus of future research.

Although our *in vitro* experiments uncover a novel mechanism by which SREBF2 enhances fibroblast proliferation in keloids through enrichment at the MDFI enhancer, it should be noted that these findings are currently limited to the cellular level. Therefore, developing a reliable *in vivo* keloid model for further validation will be a key priority in our future research.

Conclusion

In summary, based on our analysis outcomes, we demonstrate that the inhibition of SREBF2 enrichment at the MDFI enhancer reduces the hyperproliferation of KFs. This finding unveils a novel transcription factor-enhancer axis and shifts the perspective from a "gene-centered" to an "epigenetic-centered" regulatory model, revealing that the dysregulation of the SREBF2-MDFI enhancer axis is a fundamental epigenetic switch driving keloid formation. SREBF2 depletion acts as a molecular brake on keloid pathogenesis, providing new insights into the molecular regulation of KF proliferation and highlighting a potential therapeutic strategy for keloid.

Availability of Data and Materials

The analyzed data sets generated during the study are available from the corresponding author on reasonable request.

Author Contributions

CW and CH designed the research study; CW performed the research; CH collected and analyzed the data. CW has been involved in drafting the manuscript and both authors have been involved in revising it critically for important intellectual content. Both authors gave final approval of the version to be published. Both authors have participated sufficiently in the work to take public responsibility for appropriate portions of the content and agreed to be accountable for all aspects of the work in ensuring that questions related to its accuracy or integrity are addressed.

Ethics Approval and Consent to Participate

The study protocol was reviewed and approved by the Ethics Committee of Wu's Logic Aesthetics Clinic ((Research) 2025- Ethics Approval -123).

Acknowledgment

Not applicable.

Funding

This research received no external funding.

Conflict of Interest

The authors declare no conflict of interest.

References

[1] Lv W, Ren Y, Hou K, Hu W, Yi Y, Xiong M, *et al*. Epigenetic modification mechanisms involved in keloid: current status and prospect. Clinical Epigenetics. 2020; 12: 183. https://doi.org/10.1186/s13148-020-00981-8.

[2] Limandjaja GC, Belien JM, Scheper RJ, Niessen FB, Gibbs S. Hypertrophic and keloid scars fail to progress from the $CD34^{-}$/α-smooth muscle actin (α-SMA)$^{+}$ immature scar phenotype and show gradient differences in α-SMA and p16 expression. The British Journal of Dermatology. 2020; 182: 974–986. https://doi.org/10.1111/bjd.18219.

[3] Luo L, Li J, Liu H, Jian X, Zou Q, Zhao Q, *et al*. Adiponectin Is Involved in Connective Tissue Growth Factor-Induced Proliferation, Migration and Overproduction of the Extracellular Matrix in Keloid Fibroblasts. International Journal of Molecular Sciences. 2017; 18: 1044. https://doi.org/10.3390/ijms18051044.

[4] Liu S, Yang H, Song J, Zhang Y, Abualhssain ATH, Yang B. Keloid: Genetic susceptibility and contributions of genetics and epigenetics to its pathogenesis. Experimental Dermatology. 2022; 31: 1665–1675. https://doi.org/10.1111/exd.14671.

[5] Ogawa R. Keloid and Hypertrophic Scars Are the Result of Chronic Inflammation in the Reticular Dermis. International Journal of Molecular Sciences. 2017; 18: 606. https://doi.org/10.3390/ijms18030606.

[6] Asai M, Koike Y, Kuwatsuka Y, Yagi Y, Kashiyama K, Tanaka K, *et al*. Multifaceted array-based keloidal gene expression profiling reveals specific MDFI upregulation in keloid lesions. Clinical and Experimental Dermatology. 2021; 46: 1255–1261. https://doi.org/10.1111/ced.14698.

[7] Zhang M, Chen H, Qian H, Wang C. Characterization of the skin keloid microenvironment. Cell Communication and Signaling: CCS. 2023; 21: 207. https://doi.org/10.1186/s12964-023-01214-0.

[8] Ranti I, Wahyuningsih MSH, Wirohadidjojo YW. The antifibrotic effect of isolate tagitinin C from tithonia diversifolia (Hemsley) A. Gray on keloid fibroblast cell. The Pan African Medical Journal. 2018; 30: 264. https://doi.org/10.11604/pamj.2018.30.264.9994.

[9] Li Q, Cheng F, Zhou K, Fang L, Wu J, Xia Q, *et al*. Increased sensitivity to TNF-α promotes keloid fibroblast hyperproliferation by activating the NF-κB, JNK and p38 MAPK pathways. Experimental and Therapeutic Medicine. 2021; 21: 502. https://doi.org/10.3892/etm.2021.9933.

[10] Yu X, Zhu X, Xu H, Li L. Emerging roles of long non-coding

RNAs in keloids. Frontiers in Cell and Developmental Biology. 2022; 10: 963524. https://doi.org/10.3389/fcell.2022.963524.

[11] Zhou T, Chen Y, Wang C, Huang Z, Tan Z, Ma Y. SIRT6 Inhibits the Proliferation and Collagen Synthesis of Keloid Fibroblasts through MAPK/ERK Pathway. Discovery Medicine. 2024; 36: 1430–1440. https://doi.org/10.24976/Discov.Med.202436186.133.

[12] Huang B, Jiao Y, Zhu Y, Ning Z, Ye Z, Li QX, *et al*. Mdfi Promotes C2C12 Cell Differentiation and Positively Modulates Fast-to-Slow-Twitch Muscle Fiber Transformation. Frontiers in Cell and Developmental Biology. 2021; 9: 605875. https://doi.org/10.3389/fcell.2021.605875.

[13] Chen P, Quan Z, Song X, Gao Z, Yuan K. *MDFI* is a novel biomarker for poor prognosis in LUAD. Frontiers in Oncology. 2022; 12: 1005962. https://doi.org/10.3389/fonc.2022.1005962.

[14] Wang G, Wang F, Meng Z, Wang N, Zhou C, Zhang J, *et al*. Uncovering potential genes in colorectal cancer based on integrated and DNA methylation analysis in the gene expression omnibus database. BMC Cancer. 2022; 22: 138. https://doi.org/10.1186/s12885-022-09185-0.

[15] Shotorbani PY, Chaudhari S, Tao Y, Tsiokas L, Ma R. Inhibitor of myogenic differentiation family isoform a, a new positive regulator of fibronectin production by glomerular mesangial cells. American Journal of Physiology. Renal Physiology. 2020; 318: F673–F682. https://doi.org/10.1152/ajprenal.00508.2019.

[16] Wu W, Xie F, Zhang Y, Wang X, Xia L, Wu X, *et al*. A novel regulatory function for miR-217 targetedly suppressing fibronectin expression in keloid fibrogenesis. International Journal of Clinical and Experimental Pathology. 2018; 11: 1866–1877.

[17] García-García AB, Martínez-Hervás S, Vernia S, Ivorra C, Pulido I, Martín-Escudero JC, *et al*. A Very Rare Variant in *SREBF2*, a Possible Cause of Hypercholesterolemia and Increased Glycemic Levels. Biomedicines. 2022; 10: 1178. https://doi.org/10.3390/biomedicines10051178.

[18] Ma J, Chen J, Xue K, Yu C, Dang E, Qiao H, *et al*. LCN2 Mediates Skin Inflammation in Psoriasis through the SREBP2–NLRC4 Axis. The Journal of Investigative Dermatology. 2022; 142: 2194–2204.e11. https://doi.org/10.1016/j.jid.2022.01.012.

[19] Huang RL, Liu C, Fu R, Yan Y, Yang J, Wang X, *et al*. Downregulation of PLK4 expression induces apoptosis and G0/G1-phase cell cycle arrest in keloid fibroblasts. Cell Proliferation. 2022; 55: e13271. https://doi.org/10.1111/cpr.13271.

[20] Sengupta D, Kannan A, Kern M, Moreno MA, Vural E, Stack B, Jr, *et al*. Disruption of BRD4 at H3K27Ac-enriched enhancer region correlates with decreased c-Myc expression in Merkel cell carcinoma. Epigenetics. 2015; 10: 460–466. https://doi.org/10.1080/15592294.2015.1034416.

[21] Maren NA, Duduit JR, Huang D, Zhao F, Ranney TG, Liu W. Stepwise Optimization of Real-Time RT-PCR Analysis. Methods in Molecular Biology (Clifton, N.J.). 2023; 2653: 317–332. https://doi.org/10.1007/978-1-0716-3131-7_20.

[22] Schaffner W. Enhancers, enhancers - from their discovery to today's universe of transcription enhancers. Biological Chemistry. 2015; 396: 311–327. https://doi.org/10.1515/hsz-2014-0303.

[23] Klimentova EA, Suchkov IA, Shchulkin AV, Glazkova AP, Kalinin RE. Expression of Apoptotic Markers Bcl-2 and Bax in the Vascular Wall. Sovremennye Tekhnologii V Meditsine. 2021; 13: 46–50. https://doi.org/10.17691/stm2021.13.2.05.

[24] Wang Q, Wang P, Qin Z, Yang X, Pan B, Nie F, *et al*. Altered glucose metabolism and cell function in keloid fibroblasts under hypoxia. Redox Biology. 2021; 38: 101815. https://doi.org/10.1016/j.redox.2020.101815.

[25] Deng CC, Hu YF, Zhu DH, Cheng Q, Gu JJ, Feng QL, *et al*. Single-cell RNA-seq reveals fibroblast heterogeneity and increased mesenchymal fibroblasts in human fibrotic skin diseases. Nature Communications. 2021; 12: 3709. https://doi.org/10.1038/s41467-021-24110-y.

[26] McGinty S, Siddiqui WJ. Keloid. StatPearls Publishing: Treasure Island (FL). 2022.

[27] Shi K, Qiu X, Zheng W, Yan D, Peng W. MiR-203 regulates keloid fibroblast proliferation, invasion, and extracellular matrix expression by targeting EGR1 and FGF2. Biomedicine & Pharmacotherapy = Biomedecine & Pharmacotherapie. 2018; 108: 1282–1288. https://doi.org/10.1016/j.biopha.2018.09.152.

[28] Jeon YR, Roh H, Jung JH, Ahn HM, Lee JH, Yun CO, *et al*. Antifibrotic Effects of High-Mobility Group Box 1 Protein Inhibitor (Glycyrrhizin) on Keloid Fibroblasts and Keloid Spheroids through Reduction of Autophagy and Induction of Apoptosis. International Journal of Molecular Sciences. 2019; 20: 4134. https://doi.org/10.3390/ijms20174134.

[29] Vafaeie F, Nomiri S, Ranjbaran J, Safarpour H. ACAN, MDFI, and CHST1 as Candidate Genes in Gastric Cancer: A Comprehensive Insilco Analysis. Asian Pacific Journal of Cancer Prevention: APJCP. 2022; 23: 683–694. https://doi.org/10.31557/APJCP.2022.23.2.683.

[30] Sui Y, Li X, Oh S, Zhang B, Freeman WM, Shin S, *et al*. Opposite Roles of the JMJD1A Interaction Partners MDFI and MDFIC in Colorectal Cancer. Scientific Reports. 2020; 10: 8710. https://doi.org/10.1038/s41598-020-65536-6.

[31] Mi C, Zhao Y, Ren L, Zhang D. Inhibition of MDFI attenuates proliferation and glycolysis of Helicobacter pylori-infected gastric cancer cells by inhibiting Wnt/β-catenin pathway. Cell Biology International. 2022; 46: 2198–2206. https://doi.org/10.1002/cbin.11907.

[32] Xu X, Lai Y, Hua ZC. Apoptosis and apoptotic body: disease message and therapeutic target potentials. Bioscience Reports. 2019; 39: BSR20180992. https://doi.org/10.1042/BSR20180992.